The protection of indolealkylamines from LPS-induced inflammation in zebrafish

Yu Zhang[a], Norio Takagi[b], Bo Yuan[b,1], Yanyan Zhou[a], Nan Si[a], Hongjie Wang[a], Jian Yang[a], Xiaolu Wei[a], Haiyu Zhao[a,*], Baolin Bian[a,**]

[a] Institute of Chinese Materia Medica, China Academy of Chinese Medical Sciences, Beijing, 100700, China
[b] Department of Applied Biochemistry, Tokyo University of Pharmacy & Life Sciences, 1432-1 Horinouchi, Hachioji, Tokyo, 192-0392, Japan

ARTICLE INFO

ABSTRACT

Ethnopharmacological relevance: Toad skin came from *Bufo bufo gargarizans* Cantor and *Bufo melanostictus* Schneider. As the traditional Chinese medicine, it had the effect of clearing away heat and detoxification. In traditional applications, toad skin was often used for the treatment of cancer and inflammation. Total indolealkylamines (IAAs) from this medicine were proved the main compounds exert anti-inflammatory activity in our previous research.
Aim of the study: In the present study, we aimed to investigate the potential mechanism of anti-inflammatory activity of IAAs on LPS induced zebrafish.
Materials and methods: LPS induced zebrafish was applicated as an *in vivo* inflammation model to clarify the structure-activity relationship of 4 major IAAs (N-methyl serotonin, bufotenine, dehydrobufotenine and bufothionine) from toad skin. Quantitative RT-PCR was applied to detect key cytokines and members of the MyD88-dependent signaling pathway. In addition, the targeted lipidomics was conducted to find out the potential biomarkers in the inflammatory zebrafish. Network pharmacology was used to unveil the main enzymes closely related to the target lipids.
Results: Our results showed that the anti-inflammatory activity of free IAAs (N-methyl serotonin, bufotenine and dehydrobufotenine) was more potent than that of combined IAAs (bufothionine). RT-PCR demonstrated that 4 IAAs exerted antiendotoxin inflammatory effect via suppressing the TLR4/MyD88/NF-κB and TLR4/MyD88/MAPKs signaling pathway. A total of 33 possible inflammatory biomarkers, including 14 SM, 6 Cer, 11 PC and 2 GlcCer, triggered by LPS were screened out. The levels of most of candidates could be regulated toward a normal level by IAAs, especially in N-methyl serotonin and dehydrobufotenine groups. Enzymes especially LBP, PLA$_2$, CERK, SMPD and SGMS were found closely associated with the regulation of most lipid markers.
Conclusions: Overall, the mechanism underlying the anti-inflammatory activity of IAAs probably attributed to their capability to suppress NF-κB and MAPKs inflammatory pathway. Meanwhile, IAAs could also interfere the metabolism of SM, Cer and PC probably by regulating LBP, PLA$_2$, CERK, SMPD and SGMS.

1. Introduction

Toad skin came from *Bufo bufo gargarizans* Cantor and *Bufo melanostictus* Schneider. As the traditional Chinese medicine, it had the effect of clearing away heat and detoxification. In traditional applications, toad skin was often used for the treatment of cancer and inflammation (Chen et al., 2016; Qi et al., 2014). Recently, our research group proved that the hydrophilic ingredients total indolealkylamines

(IAAs) from toad skin displayed good anti-inflammatory activity in LPS-stimulated zebrafish (Zhang et al., 2019). However, the mechanism underlying its anti-inflammatory activity is far from being understood.

As we know, LPS recognized toll-like receptor 4 (TLR4) on the surface of the cell membrane specificity (Liang et al., 2018; Yang et al., 2017). Subsequently activated myeloid differentiation factor 88 (MyD88) or TIR-domain-containing adapter-inducing interferon-β (TRIF) signaling pathway (Dong et al., 2018; GM and R, 2003; Wang

---

et al., 2015). Nuclear Factor-kappa B (NF-κB) and mitogen-activated protein kinase (MAPKs) were two classic inflammatory signaling pathways downstream of MyD88-dependent pathway (GM and R, 2003; Ryu et al., 2015). Activation of NF-κB pathway resulted in the release of pro-inflammatory factors, like IL-1β, IL-6, TNF-α (Hwang et al., 2018). Directly inhibition of these cytokines was considered a good strategy to relieve inflammation (Hwang et al., 2016).

Also, the lipids serve as a key participant in the inflammation response (Dressler et al., 1992; Heller and Krönke, 1994; Kim et al., 1991; Lim et al., 2015; Titz et al., 2018). Pro-inflammatory cytokines such as TNF-α led to changes of many lipids, especially phosphatidylcholines (PC), sphingomyelin (SM) and its metabolites (Maceyka and Spiegel, 2014). Lipidomics improved greatly in recent years due to the development of mass spectrometry (MS) technology (Han and Gross, 2003), which were applied for the discovery of biomarkers to support diagnosis and treatment monitoring. Novel applications of lipidomics in the biomedical sciences have emerged, such as metabolic syndrome, neurological disorders, cancer, drug discovery and screens (Han, 2005; Meikle et al., 2014; Murph et al., 2007; Wenk, 2005; Yang and Han, 2016; Zhao et al., 2014).

With the advent of the continuous accumulation of omics data and the progress of bioinformatics methods, network pharmacology has been used in lots of study and made it possible to analyze the systematic relationship between proteins and endogenous ingredients (Zhang et al., 2018; Zheng et al., 2018).

In this study, LPS mediated transgenic fluorescent zebrafish were applied to assess the structure-activity relationship of 4 major IAAs isolated from toad skin (Zhang et al., 2019). The expression levels of inflammatory mediators downstream of MyD88 were determined to explore the anti-inflammatory mechanism of IAAs. Lipidomics technique was carried out to investigate the regulation function of lipid homeostasis of IAAs. Furthermore, A network of lipids-enzymes was constructed to uncover the potential therapeutic targets of IAAs on LPS mediated inflammation, thus to pinpoint medicinal value of IAAs.

2. Materials and Methods

2.1. Chemical and reagents

MS grade formic acid (A117-50), acetonitrile (A955-4) and methanol (A456-4) and Deionized water (W6-4) were obtained from Fisher Scientific (Fair Lawn, NJ, USA); ammonium acetate (238074-25G) was purchased from Sigma-Aldrich Co. (St. Louis, MO, USA); other chemicals and solvents were of analytical grade. LPS, dimethyl sulfoxide (DMSO), and methyl cellulose were purchased from Sigma-Aldrich Co. (St. Louis, MO, USA).

The reference standards, including N-methyl serotonin, bufotenine, dehydrobufotenine and bufothionine, were isolated from the crude extract of toad skin in the preliminary experiment. The details of extraction and isolation was shown as follows: The dried toad skin (5 kg) were extracted with water (20 L × 3) at room temperature. After concentration of the combined extract under reduced pressure, the residue (200 g) was mixed with ODS (200 g). The sample mixture was subjected to ODS C_{18} and eluted with 2 L water (Fir.1) and 2 L 30% methanol (Fir.2). Fir.2 (30 g) was separated by preparative HPLC (Ace/0.1% acetic acid-water, 8:92, v/v) to yield 4 IAAs. After compared the NMR and LC-HR-MS spectrum with literature reported before, the structure of 4 IAAs was identified as N-methyl serotonin, bufotenine, dehydrobufotenine and bufothionine. The purities of these standards were above 98% according to HPLC-UV analysis. The NMR and LC-HR-MS spectrum of four standards were shown in Figure S1-S12.

2.2. Fish maintenance and care

Transgenic neutrophilic fluorescent zebrafish (10 and 12 months) of both sexes were purchased from Hunter Biotechnology, Inc.

Table 1
Quantitative PCR primer sequences.

Name	Primer	Sequence	Size
b- actin	Forward	5'- CCATCTATGAGGGTTACGC -3'	137bp
	Reverse	5'- GACAATTTCTCTTTCGGCT -3'	
TNF-α	Forward	5'- GCTGGATCTTCAAAGTCGGGTGTA -3'	139 bp
	Reverse	5'- TGTGAGTCTCAGCACACTTCCATC -3'	
IL-1β	Forward	5'- CTCAGCCTGTGTGTTTGGGA -3'	209bp
	Reverse	5'- GGGACATTTGACGGACTCG -3'	
IL-6	Forward	5'- ACGACATCAAACACAGCACC -3'	172bp
	Reverse	5'- TCGATCATCACGCTGGAGAA -3'	
MyD88	Forward	5'- ACCATCGCCAGTGAGCTTAT -3'	206bp
	Reverse	5'- CAGATGGTCAGAAAGCGCAG -3'	
ERK1	Forward	5'- TCCAAGGGCTACACCAAGTC -3'	274bp
	Reverse	5'- TGCCGATCCAATAAATCCAAA -3'	
JNK1	Forward	5'- ATTGCCTTTTGTCAGGGTTT -3'	140bp
	Reverse	5'- TACCGTTTGAGAACCGTGAA -3'	
p38a	Forward	5'- GTCGCAGAAAGAAAGACCCA -3'	130bp
	Reverse	5'- ATCAAACGCAGAGCAAACAG -3'	
IκB-α	Forward	5'- GTTGGATTCGTTAAAAGAGGA -3'	137bp
	Reverse	5'- GGATAATGGCGAGATGTAGAT -3'	
P65	Forward	5'- CGCAAGAGAACTGAAGGAA -3'	205bp
	Reverse	5'- AGAAAAAGGAGGTGGGTGG -3'	
TRIF	Forward	5'- GAGAGCGCTTGAACTGTAGC -3'	167bp
	Reverse	5'- ACCAGCCGTTTTGCATGATT -3'	
IL-10	Forward	5'- GGAGACCATTCTGCCAACA -3'	111bp
	Reverse	5'- CATTTCACCATATCCCGCT -3'	
IFN-γ	Forward	5'- GTTTGCTGTTTTCGGGATGG -3'	138bp
	Reverse	5'- TTCGCAGGAAGATGGGGTGT -3'	

(HangZhou, China). The fish maintenance and care procedure were same as the paper we published (Zhang et al., 2019), except there were 4 IAAs-treated group (N-methyl serotonin, bufotenine, dehydrobufotenine and bufothionine) with 3 concentrations (25 μg/mL, 50 μg/mL, 100 μg/mL) for 3 h at 28 °C, respectively. These larvae sample were prepared for the study of structure-activity relationship of 4 IAAs. Specifically, sample with high dosage of 4 IAAs (100 μg/mL) were prepared for further lipid profiling analysis and detection of cytokines.

2.3. RNA extraction real-time quantitative PCR

After an injection of 10 mg/mL LPS into the zebrafish larvae yolk (3df) in the absence or presence of 100 μg/mL IAAs for 3 h, total RNA was extracted using Trizol regent (Invitrogen) according to the manufacturer's instructions (Carlsbad, CA, USA). The total RNA (5 μg) was used to produce cDNA using an RT-PCR system with the conditions as follow: 2 min at 50 °C, 10 min at 95 °C, 30 s at 95 °C, 30 s at 60 °C, 40 cycles. Relative quantitation was performed by standard curves for each primer. The amount of mRNA was normalized to that of β-actin. Primers were designed for genes listed in Table 1. Data analysis was performed using the standard curve and △△Ct methods.

2.4. Lipid profiling analysis of zebrafish larvae

After treated with different IAAs, zebrafish larvae were fitted in centrifuge tube with each tube for 2, subsequently 600 μL chloroform/methanol (3:1) was added. Then the ultrasound was done for 10 min, followed by vortex for 2 h. Subsequently, added 100 μL water and mixed thoroughly. After centrifugation at 4 °C for 10 min at 12000 rpm, 300 μL subnatant was taken and dry, then added 400 μL isopropyl alcohol/acetonitrile (1:1), dissolved in ultrasound. Repeat the previous centrifugal operation, then transferred 100 μL supernatant for UPLC-MS analysis. The Total ion chromatograms (TIC) of zebrafish sample was shown in Fig. S13.

The sample analysis was performed by UltiMate™3000 Rapid Separation LC (RSLC) system (Thermo Scientific, USA). An ACQUITY UPLC HSS T3 C18 column (1.8 mM, 100 × 2.1 mm, Waters™, USA) was

applied for compound retention. The mobile phase A was acetonitrile/water (60/40) and mobile phase B was isopropanol/acetonitrile (90/10); both A and B contained 0.1% formic acid and 10 mmol/L ammonium acetate with a gradient elution (0–2 min, 20–30% B; 2–5 min, 30–45% B; 5–6.5 min, 45–60% B; 6.5–12 min, 60–65% B; 12–14 min, 65–85% B; 14–17.5 min, 85–100% B; 17.5–18 min, 100-100% B). The re-equilibration was 2 min with 20% B. The flow rate of the mobile phase was 0.3 mL/min. The column temperature was maintained at 45 ˚C and the sample manager temperature was set at 4 ˚C.

A Thermo Scientific™ Q Exactive™ hybrid quadrupole Orbitrap mass spectrometer equipped with a HESI-II probe was employed in the positive electrospray ionization mode. The pos HESI-II spray voltages were 3.7 kV, the heated capillary temperature was 320 ˚C, the sheath gas pressure was 30 psi, the auxiliary gas setting was 10 psi, and the heated vaporizer temperature was 300 ˚C. Both the sheath gas and the auxiliary gas were nitrogen. The collision gas was also nitrogen at a pressure of 1.5 mTorr. The parameters of the full mass scan were as follows: a resolution of 70,000, an auto gain control target under 1×10^6, a maximum isolation time of 50 ms, and an m/z range 50–1500 Da.

2.5. Data processing and statistical analysis

The raw LC-MS data was imported to the Skyline software (http://skyline.gs.washington.edu/) for the relative quantification of the lipid species according to the retention time and accurate mass in the constructed lipids database. Briefly, the work flow for using Skyline for the analysis of 118 targeted lipids consisted of the following steps: (1) flat file containing the 118 molecules; (2) import the small molecule list into the Skyline, building an analysis template; (3) import the raw data. The chromatographic data for each lipid were manually analyzed to determine the quality of the signal and peak shape. Before chemometrics analysis, all of the detected ion signals in each sample were normalized to the obtained total ion count value. Statistical significance was determined by one-way ANOVA followed by Tukey multiple comparison test or Student's t-tests. A value of $P < 0.05$ was considered to be statistically significant.

2.6. Interaction and network visualization of lipid markers and enzymes

HMDB datebase (http://www.hmdb.ca/) was used to screen out the enzymes which involved in the metabolism of lipid markers. Network visualization of biomarkers and enzymes was performed using Cytoscape v3.7.1 (National Resource for Network Biology, Bethesda, MD, USA). Network Analyzer plug-in was used for Network topology analysis, with the connection degree > 10 (play a key role in the Network) to construct the interaction network diagram of "lipids-enzymes ".

3. Results

3.1. Structure-activity relationship of 4 IAAs

Our previous study preliminary proved the anti-inflammatory activity of total IAAs. In order to clarify the structure-activity relationship, 4 major IAAs (N-methyl serotonin, bufotenine, dehydrobufotenine, and bufothionine) with different substituent group were selected to compare their effect at low, medium and high dosage (25, 50, 100 μg/mL) in LPS-stimulated zebrafish (Zhang et al., 2019).

According to Fig. 1-A, the number of neutrophil in the yolk sac of model group (18) was significantly increased compared with control group (CG) (3). After the administration of positive medicine indomethacin (Indo) and 4 IAAs, the number of neutrophil was reduced in different degrees. A dose-dependent relationship was obtained by 4 IAAs at three dosage. Specifically, when the concentration was 25 μg/mL, the number of neutrophils in 4 treated groups was 12, 12, 11 and

17 (Fig. 1-B), with the anti-inflammatory effects on zebrafish were 37%, 37%, 42% and 11%, respectively. While, when the dose was 100 μg/mL, the activity reached 58%, 53%, 58% and 37%, respectively (Fig. 1-C). The anti-inflammatory activity of the positive medicine indomethacin was 26% when the concentration was 28.6 μg/mL.

3.2. Effect of IAAs on the mRNA expression of 12 inflammatory mediators

A total of 12 inflammatory mediators were detected from mRNA level, including 2 proteins triggered by TIR4 (MyD88 and TRIF), 5 protein in NF-κB and MAPK pathways (IκB-α, p65, ERK1, JNK1 and p38α) and 5 inflammatory cytokines (IL-1β, IL-6, TNF-α, IFN-γ and IL-10).

As shown in Fig. 2, compared with control group, the mRNA level of IL-1β, IL-6, TNF-α and IFN-γ were significantly increased in LPS-treated larvae ($P < 0.001$), the expression of IL-10 was markedly reduced ($P < 0.01$). In the administration groups, all the 4 IAAs could regulate the expression of these cytokines toward a normal level, especially for N-methyl serotonin and bufotenine ($P < 0.01$).

The expression of MyD88 and TRIF significantly upregulated in LPS treated zebrafish compared with those in control group ($P < 0.001$), indicating both pathways downstream of TLR4 were activated. In addition, after treated with 4 IAAs, N-methyl serotonin showed an obvious regulation ability than other IAAs.

The results also revealed that the expression of IκB-α was significantly decreased and p65 was increased in LPS-stimulated zebrafish ($P < 0.001$). The mRNA level of ERK1, JNK1 and P38α displayed significant downtrend in LPS group ($P < 0.001$). NF-κB pathway relied on IKK-mediated IκB-α phosphorylation. Subsequently allowed the p50/p65 NF-κB dimer to enter the nucleus and activate gene transcription (Kim-Anne et al., 2011; Zong et al., 2015).

3.3. Lipid profiling analysis and identification of potential biomarkers

In order to find out the potential inflammatory markers, targeted lipidomics was carried out in this study. Generated targeted database (contains more than 200 lipids) was used to identify the lipids in LPS mediated zebrafish samples based on retention time and accurate mass values. At last, 118 lipids were detected (Table S1), including 72 phosphatidylcholines (PC), 18 phosphatidylethanolamine (PE), 15 sphingomyelin (SM),10 ceramide (Cer) and 3 glucosylceramide (GlcCer).

The significantly changed lipids between model group (LPS) and control group were filtered out based on t-test ($P < 0.05$). A total of 33 possible inflammatory biomarkers including 14 SM, 6 Cer, 11 PC and 2 GlcCer were screened out. The changed levels and names of the biomarkers were shown in Fig. 3. All of them were found significantly increased in model group compared with control group ($P < 0.05$). After the treatment of IAAs, most of these pathological markers could be down-regulated by N-methyl serotonin and dehydrobufotenine. Only a few were regulated by bufotenine and bufothionine.

After the comparison of the contents of 118 known lipids between administration groups and model group, t-test (t < 0.05) was used as the screening criteria for differential lipids. A total of 37 lipids were down-regulated by N-methyl serotonin, including 13 SM, 3 Cer, 14 PC and 7 PE, among which 12 SM, 3 Cer and 9 PC were pathological marker. Dehydrobufotenine could down-regulate 101 lipids, including 14 SM, 8 Cer, 3 GlcCer, 62 PC and 14 PE, with12 SM, 3 Cer and 11 PC were identical with pathological markers. While, only 2 Cer were regulated by bufotenine. As for bufothionine, there were 60 lipids were screened out, including 3 Cer, 48 PC and 9 PE. However, only 1 Cer and 3 PC were pathologic marker.

3.4. Lipids-enzymes network visualization analysis

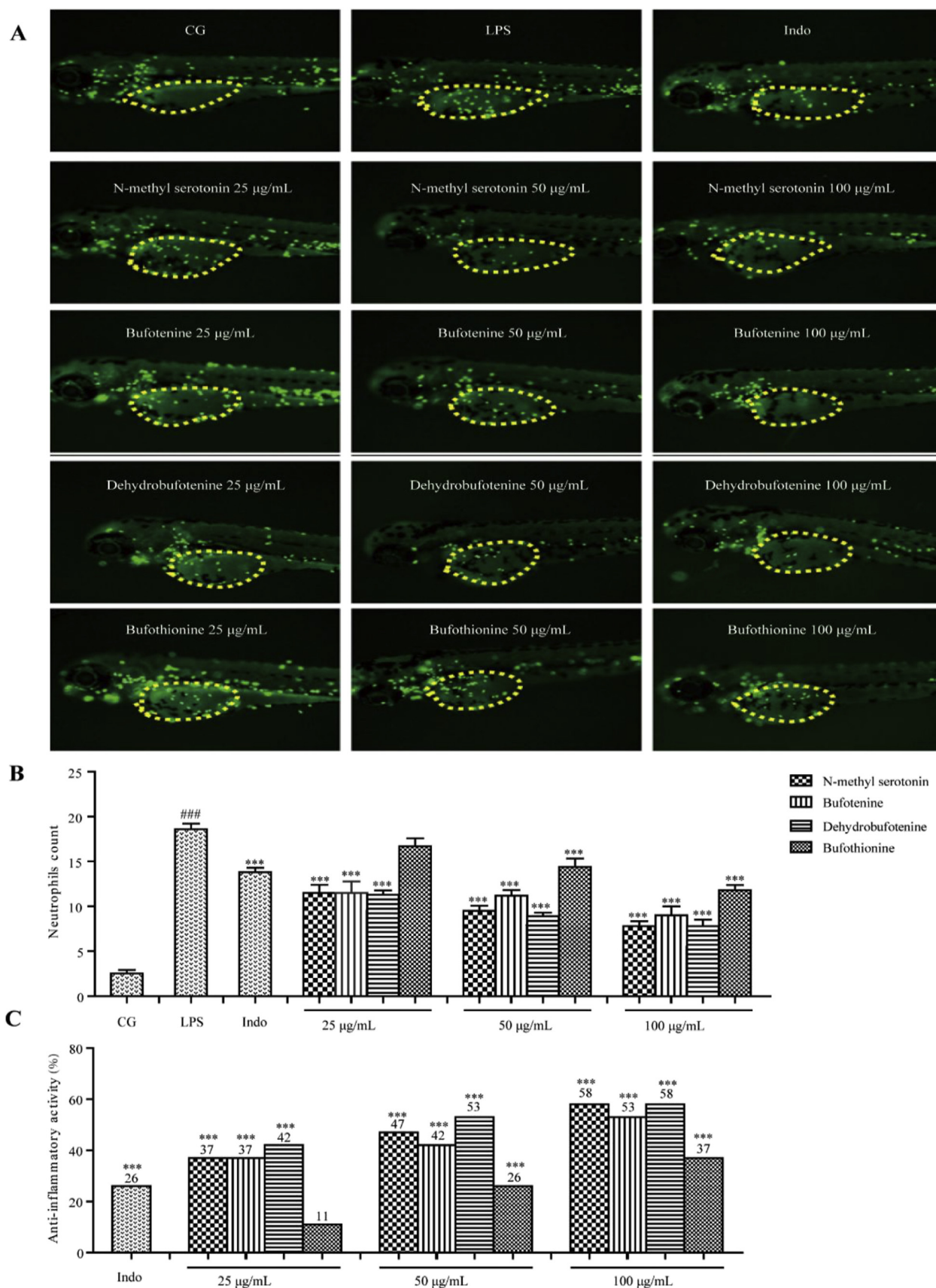In order to build a more systematic lipid metabolism network, a

Fig. 1. N-methyl serotonin, bufotenine, dehydrobufotenine and bufothionine inhibits neutrophil recruitment induced by LPS; Fluorescence imaging of 3-dpf zebrafish live larvae (n = 10). The green dot in yellow circle indicates the neutrophil. The CG, LPS and Indo group (28.6 μg/mL) are shown (A). B and C show the number of neutrophil and inflammatory activity in each group, respectively. ***$P < 0.001$, **$P < 0.01$, *$P < 0.05$, compared with LPS group. (For interpretation of the references to colour in this figure legend, the reader is referred to the Web version of this article.)
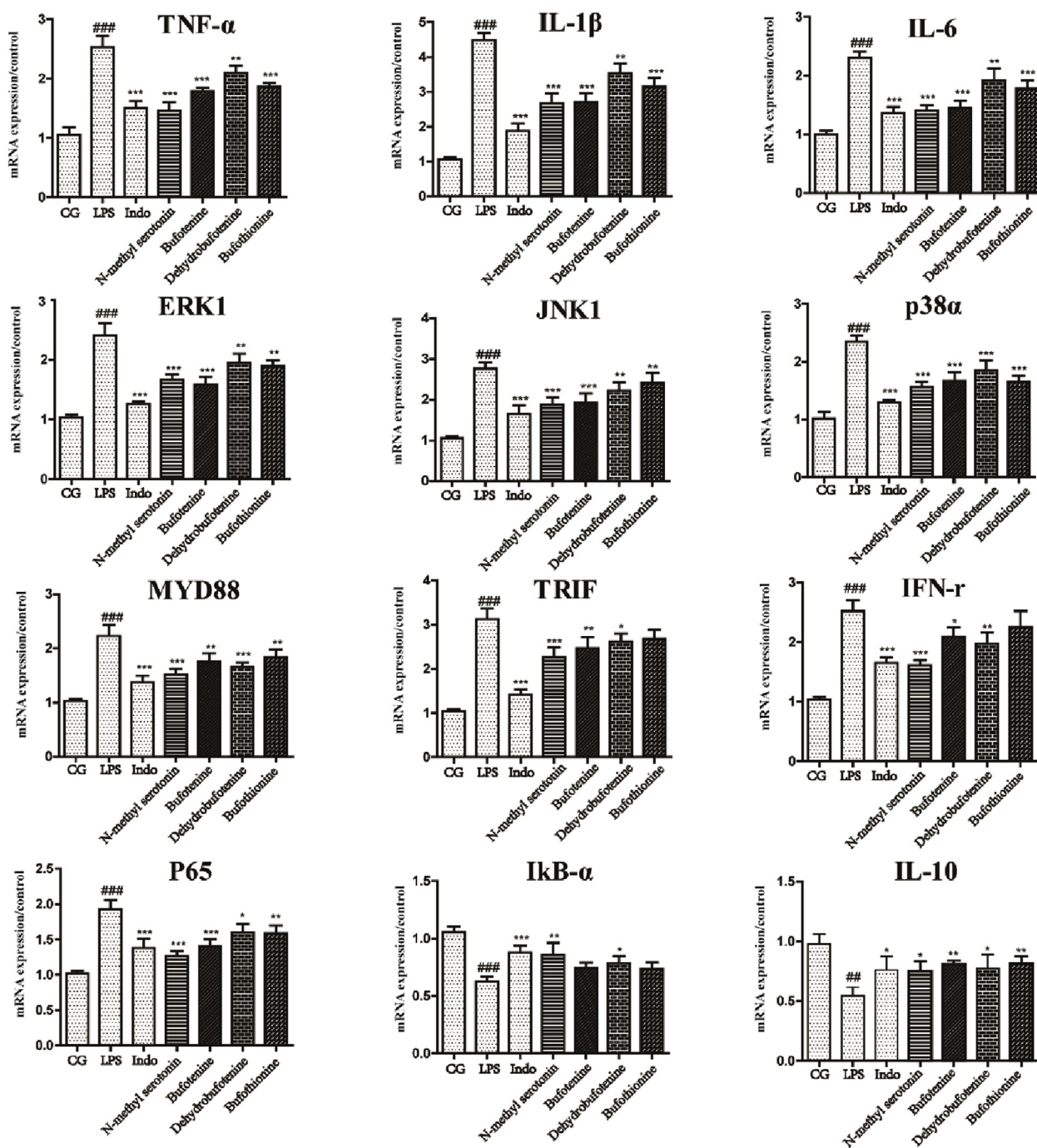
Fig. 2. 4 AIIs inhibits LPS-induced inflammation by suppressing TLR4/MyD88/NF-κB and TLR4/MyD88/MAPK signaling pathway.

diagram consisting of inflammatory biomarkers and lipid enzymes was constructed by Cytoscape software. All the enzymes were downloaded from HMDB database. As shown in Fig. 4, a total of 26 predicted targets enzymes involved in the regulation of lipid markers were screened out, based on the topological features (targets with greater degree, betweenness and closeness than the median).Among these enzymes, phospholipase A_2 (PLA$_2$) and lysophosphatidylcholine acyltransferase (LPCAT) were shown related to the metabolism of PC. LPS-binding protein (LBP) and sphingomyelin phosphodiesterase (SMPDs) were shown associated with the metabolism of SM and Cer. Sphingolipid synthetase (SGMS) were shown involved in the metabolism of PC, SM and Cer.

4. Discussion

The anti-inflammatory activities of N-methyl serotonin, bufotenine and dehydrobufotenine were stronger than that of bufothionine. Bufothionine was a kind of combined IAA with a sulfate radical attached to the C-5 position. The rest of other IAAs were free IAAs with the C-5 position replaced by hydroxyl group. Thus, we speculated that the hydroxyl in the C-5 was an active group. Once 5-OH was replaced by sulfate radical, the anti-inflammatory activity reduced significantly. Therefore, whether 5-OH was substituted or not influenced on the activity of these compounds closely. In addition, quaternary amines should be another important factor associated with the anti-inflammatory activity of IAAs, that was maybe the reason why the effect of dehydrobufotenine (quaternary amines alkaloid) was best among the
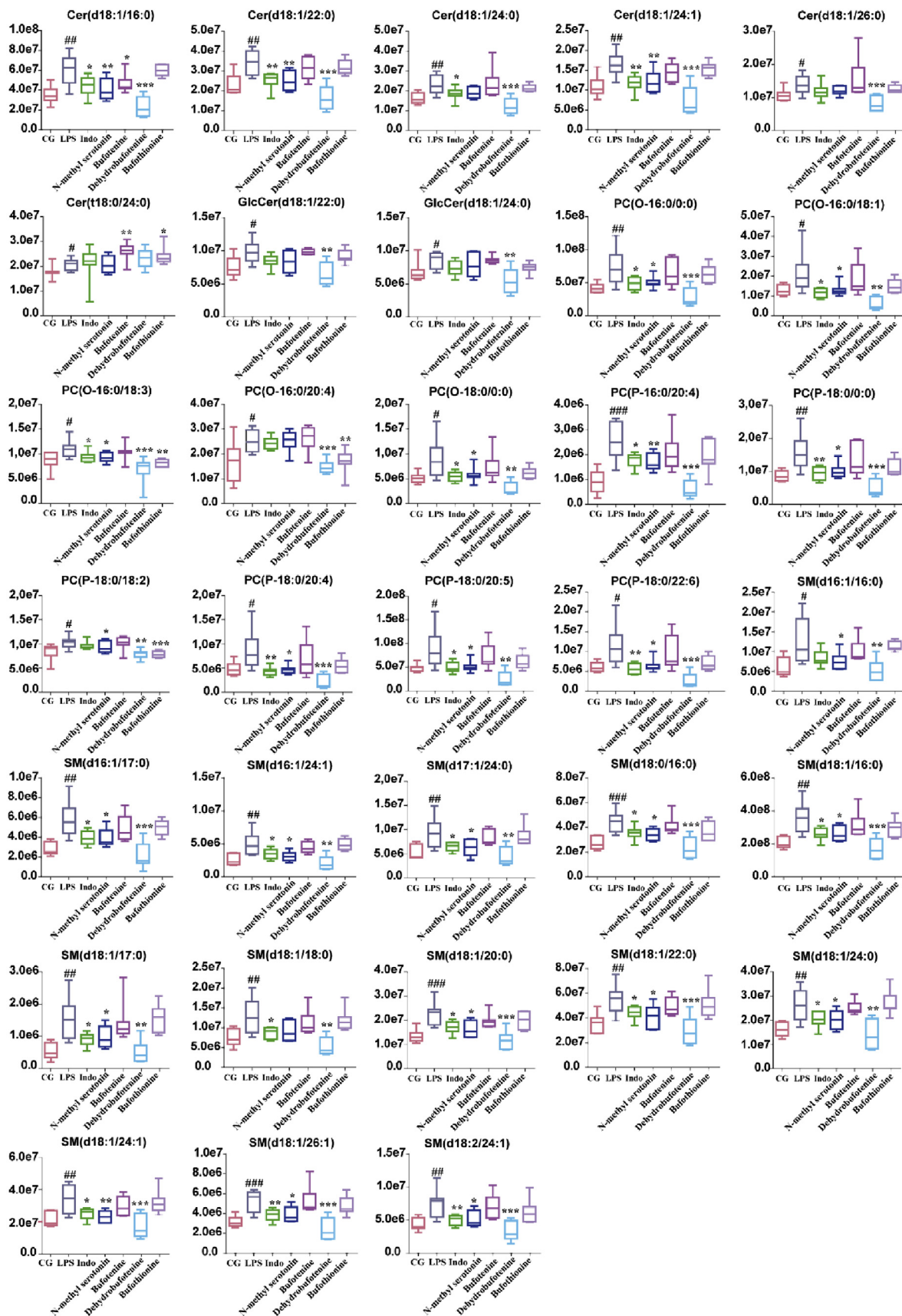
5

Fig. 3. Metabolic changes of lipids in the seven groups. #P < 0.05, ##P < 0.01, ###P < 0.001 the model group versus the control group; *P < 0.05, **P < 0.01, ***P < 0.001 the treated group and positive group versus the model group.
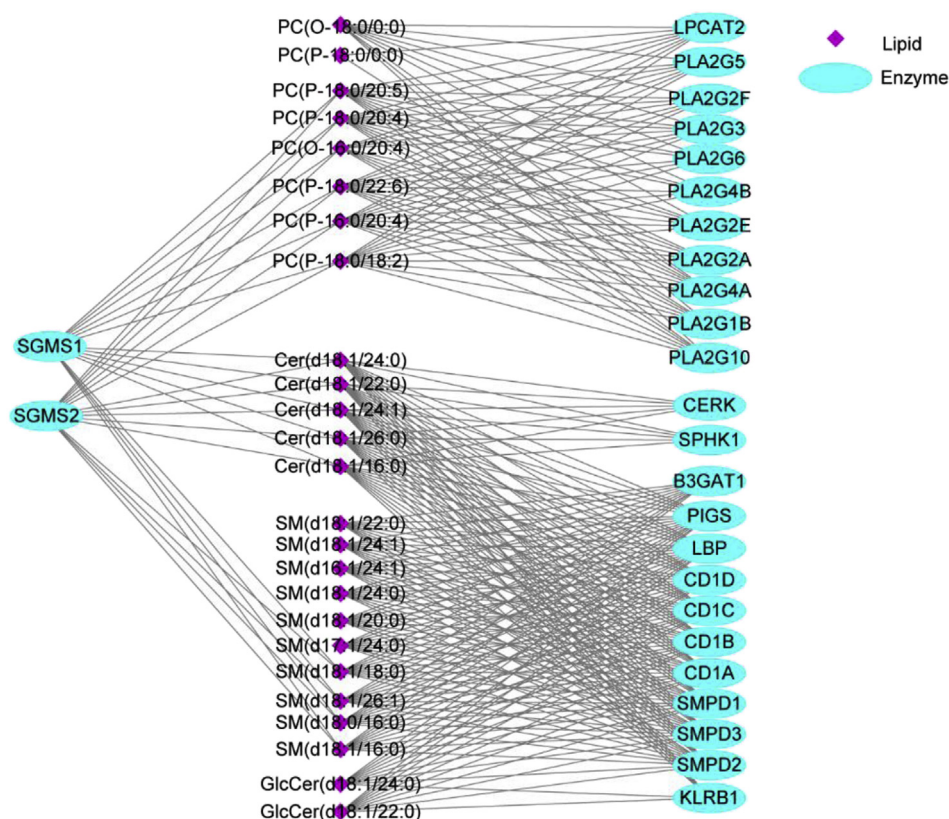
Fig. 4. Network of interactions between lipid markers and enzymes. Purple nodes represent lipid markers, blue nodes represent enzymes. (For interpretation of the references to colour in this figure legend, the reader is referred to the Web version of this article.)

3 free IAAs.

The results of RT-PCR suggested that both NF-κB and MAPK pathways in this study were activated (Zong et al., 2015). Cytokines mentioned in this study toward to a normal level after treated with 4 IAAs, especially N-methyl serotonin($P < 0.01$). Which means that 4 IAAs attenuated the inflammation possibly via suppressing the TLR4/MyD88/NF-κB and TLR4/MyD88/MAPK signaling pathways. In addition, The key factors downstream of TRIF pathway deserve further verification.

Data from targeted lipidomics showed that sphingolipids (SM and Cer) and glycerophospholipids PC were the main inflammatory markers triggered by LPS, Literatures demonstrated that SM and Cer were involved in the cell growth, proliferation, differentiation and apoptosis. More importantly, they were also associated with the regulation of inflammatory response (Cuvillier et al., 1996; Hannun, 1994; Hannun and Obeid, 1995; Kolesnick and Krönke, 1998; Li et al., 2014; Venable et al., 1995). A recent study proved that elevated plasma SM (d18:1/22:0) was closely related to hepatic steatosis in patients with chronic hepatitis C virus infection (Li et al., 2014). The glycerophospholipids PC and PE made up more than 50% of the total phospholipid in eukaryotic membranes with the important roles in the membranes structure and function (Gibellini and Smith, 2010).

We also found that the content of these lipids was elevated in model group. Previous study showed that LPS could promote the *de novo* pathway and sphingomyelin hydrolysis by activating serine palmitoyl transferase and acid sphingomyelinase *in vivo* and *in vitro*, eventually led to the elevation of Cer (Chang et al., 2011; Memon et al., 1998). Increased Cer were synthesized into SM and GluCer by sphingolipid synthetase (SGMS) and glucosylceramide synthetase (GluCerS) (Maceyka and Spiegel, 2014). The elevation of PC probably due to an upregulation in the transcription of the choline transporter-like protein 1 (CTL1) gene *(Slc44a1)*, which facilitated an increased rate of uptake and synthesis of PC (Snider et al., 2018). Generated PC could be

hydrolyzed to form diacylglycerol (DAG) under the action of phosphatidylcholine (PC)-phospholipase C (PC-PLC). DAG activated A-SMase resulting in the hydrolysis of SM to produce Cer (Schütze et al., 1992).

As for the regulation ability of 4 IAAs to lipid homeostasis, N-methyl serotonin and dehydrobufotenine could down-regulate most of pathological markers as well as other PC and PE. While, bufotenine and bufothionine only regulate little of these biomarkers. It's worth pointing out that the regulation ability on lipid markers of 4 IAAs was consistent with the trend of their anti-inflammatory activity.

Accoring to Fig. 4, PLA$_2$ and LPCAT were related to the metabolism of PC. Previous literature demonstrated that PLA$_2$ released the sn-2 fatty acid from PC to generate lysophosphatidylcholine (LPC) and arachidonic acid (AA) (Ditz et al., 2018). LPCAT catalyzed the acylation and de-acylation of both sn-positions of PC, with a preference for the sn-2 position. LBP and SMPDs were associated with the metabolism of SM and Cer. Evidence supported that increased LBP levels presumably lead to enhanced expression of SMPDs, resulting in consumption of SM and elevation of Cer, as found in adipose tissue from *ob/ob* mice (Fahumiya et al., 2006). The expression of SMase such as SMPD1, SMPD2 and especially those of SMPD3 increased with adipose tissue inflammation (Kolak, 2012). During the metabolism of sphingolipids, ceramide transport kinase (CERK) could convert Cer to C1P in a Ca^{2+}-dependent manner and activate MAPK signaling by invoking ERK1/2, JNK and p38 (Yoo et al., 2012). Besides, CERK was found to modulate NF-κB activity in neutrophils from the LPS-induced lung Injury (Newcomb et al., 2018). SGMS have also been shown associated with the metabolism of PC, SM and Cer, because of it transferred the phosphorylcholine head group from the phospholipid PC to Cer, eventually formed SM and DAG (Maceyka and Spiegel, 2014).

Diagram of possible anti-inflammatory mechanisms of IAAs was constructed. As shown in Fig. 5. After triggered by LPS, TLR4/MyD88/NF-κB and TLR4/MyD88/MAPKs signaling pathway were activated
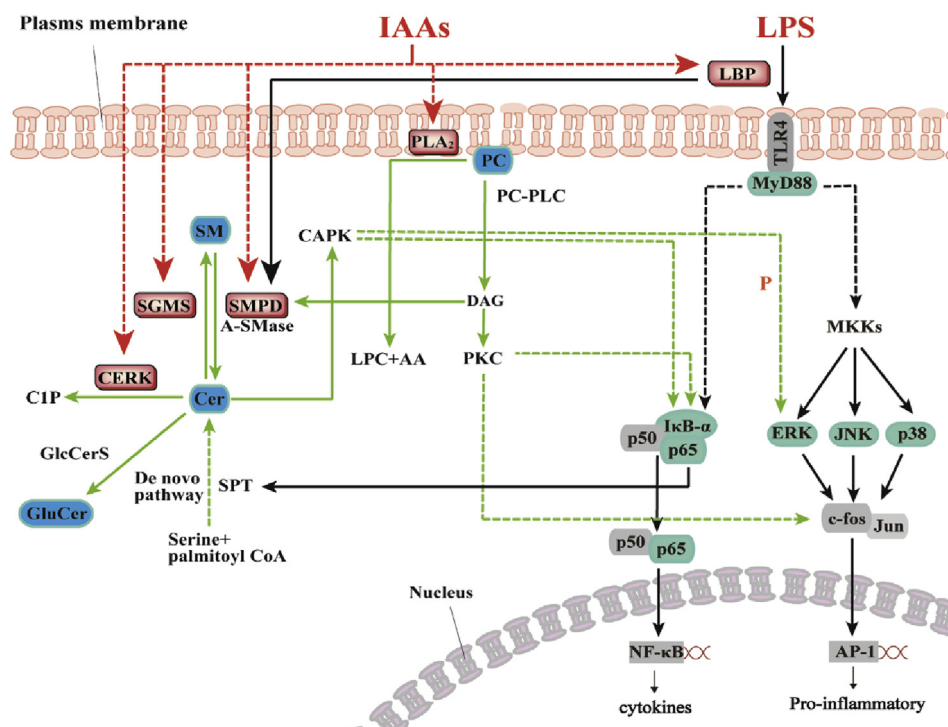
Fig. 5. The possibly anti-inflammatory mechanism of IAAs induced by LPS. IAAs down-regulated lipids of SM, Cer, GluCer and PC and suppressing the inflammation pathway of TLR4/MyD88/NF-κB and TLR4/MyD88/MAPKs probably by acting on the enzymes like LBP, PLA2, CERK, SMPD and SGMS.

combined with the elevation of SM, Cer, GlcCer and PC. Importantly, LBP, PLA$_2$, CERK, SMPD and SGMS were found the key enzymes which could affect the metabolism of lipid markers. Therefore, these enzymes probably were the potential therapeutic targets of IAAs. By regulating their activity, IAAs could further regulate the content of lipids, thus to exert an anti-inflammatory effect.

On the other hand, increased lipids like PC and Cer were reported to promote the production of inflammatory factors. For example, as a second messenger, Cer stimulated a serine/threonine ceramide-activated protein kinase (CAPK) (Schütze et al., 1992), which further phosphorylated and activated Raf-1 kinase. Activated Raf-1 could phosphorylate and stimulate a dual specificity mitogen-activated kinase (MEK-1), which eventually phosphorylated and activated extracellular signal-regulated kinases (ERKs) (Schwandner et al., 1998). In addition, Raf-1 protein kinase also activated the NF-κB transcription factor by phosphorylating the NF-κB inhibitor IκB-α (HäFner et al., 1994; Kolesnick and Golde, 1994). As a hydrolyzed product of PC, DAG could activate protein kinase C (PKC). PKC further activated NF-κB signaling pathway and mediate the induction of JUN and FOS proteins that were components of the AP-1 transcription factor (Dressler et al., 1992; Schütze et al., 1992). Besides, the overexpression of p65, an active subunit of NF-κB, could up-regulated the Cer through promoting the *de novo* pathway (Chang et al., 2011).

However, the relationship between lipids and TLR4 receptors in LPS-induced models requiring further verification.

5. Conclusions

Our study evaluated the structure-activity relationship of 4 IAAs (N-methyl serotonin, bufotenine, dehydrobufotenine and bufothionine) in transgenic fluorescent zebrafish and proved that the anti-inflammation activity of free IAAs was stronger than that of combined IAA. The mechanism of IAAs exhibited anti-inflammatory activity on LPS induced zebrafish probably by suppressing TLR4/MyD88/NF-κB and TLR4/MyD88/MAPKs signaling pathways combined with regulating lipids homeostasis of SM, Cer, GluCer and PC. Enzymes especially LBP,

PLA$_2$, CERK, SMPD and SGMS were the potential therapeutic target for IAAs to regulate lipid homeostasis and further influence the inflammation pathway.

Conflicts of interest

The authors declare no competing financial interest.

Appendix A. Supplementary data

Supplementary data to this article can be found online at https://doi.org/10.1016/j.jep.2019.112122.

Author contributions

Y.Z. performed the experiments, analyzed the data, and wrote the manuscript; N.T., B.Y. and Y.Z. performed the experiments; H.W. analyzed the data; N.S. performed the experiments; J.Y. and X.W. revised the manuscript; B.B. and H.Z. contributed to the study design and overall supervision. All authors reviewed the manuscript.

References

Chang, Z.Q., Lee, S.Y., Kim, H.J., Kim, J.R., Kim, S.J., Hong, I.K., Oh, B.C., Choi, C.S., Goldberg, I.J., Park, T.S., 2011. Endotoxin activates de novo sphingolipid biosynthesis via nuclear factor kappa B-mediated upregulation of Sptlc2. Prostaglandins Other Lipid Mediat. 94, 44–52.

Chen, T., Yuan, S.J., Yu, X.Q., Jiao, L.B., Hu, W., Chen, W.L., Xie, B., 2016. Effect of toad skin extracts on the pain behavior of cancer model mice and its peripheral mechanism

of action. Int. Immunopharmacol. 42, 90–99.

Cuvillier, O., Pirianov, G., Kleuser, B., Vanek, P.G., Coso, O.A., Gutkind, S., Spiegel, S., 1996. Suppression of ceramide-mediated programmed cell death by sphingosine-1-phosphate. Nature 381, 800–803.

Ditz, T., Schnapka-Hille, L., Noack, N., Dorow, J., Ceglarek, U., Niederwieser, D., Schiller, J., Fuchs, B., Cross, M., 2018. Phospholipase A2 products predict the hematopoietic support capacity of horse serum. Differentiation 105, 27–32.

Dong, D., Zhou, H., Na, S.Y., Niedra, R., Peng, Y., Wang, H., Seed, B., Zhou, G.L., 2018. GPR108, an NF-kappaB activator suppressed by TIRAP, negatively regulates TLR-triggered immune responses. PLoS One 13. https://doi.org/10.1371/journal.pone.0205303.

Dressler, K.A., Mathias, S., Kolesnick, R.N., 1992. Tumor necrosis factor-alpha activates the sphingomyelin signal transduction pathway in a cell-free system. Science 255, 1715–1718.

Fahumiya, S., Hester, K.D., Guang, Y., Hannun, Y.A., Jacek, B., 2006. Altered adipose and plasma sphingolipid metabolism in obesity: a potential mechanism for cardiovascular and metabolic risk. Diabetes 55, 2579–2587.

Gibellini, F., Smith, T.K., 2010. The Kennedy pathway–De novo synthesis of phosphatidylethanolamine and phosphatidylcholine. IUBMB Life 62, 414–428.

GM, B., R, M., 2003. Toll-like receptor signaling pathways. Science 300, 1524–1525.

HäFner, S.,., Adler, H.S., Mischak, H.,., Janosch, P.,., Heidecker, G.,., Wolfman, A.,., Pippig, S.,., Lohse, M.,., Ueffing, M.,., Kolch, W., 1994. Mechanism of inhibition of Raf-1 by protein kinase A. Mol. Cell. Biol. 14, 6696–6703.

Han, X., 2005. Lipid alterations in the earliest clinically recognizable stage of Alzheimer's disease: implication of the role of lipids in the pathogenesis of Alzheimer's disease. Curr. Alzheimer Res. 2, 65–77.

Han, X., Gross, R.W., 2003. Global analyses of cellular lipidomes directly from crude extracts of biological samples by ESI mass spectrometry: a bridge to lipidomics. J. Lipid Res. 44, 1071–1079.

Hannun, Y.A., 1994. The sphingomyelin cycle and the second messenger function of ceramide. J. Biol. Chem. 269, 3125–3128.

Hannun, Y.A., Obeid, L.M., 1995. Ceramide: an intracellular signal for apoptosis. Trends Biochem. Sci. 20, 73–77.

Heller, R.A., Krönke, M., 1994. Tumor necrosis factor receptor-mediated signaling pathways. J. Cell Biol. 126, 5–9.

Hwang, J.H., Kim, K.J., Ryu, S.J., Lee, B.Y., 2016. Caffeine prevents LPS-induced inflammatory responses in RAW264.7 cells and zebrafish. Chem. Biol. Interact. 248, 1–7.

Hwang, S.J., Ahn, E.Y., Park, Y., Lee, H.J., 2018. An aqueous extract of Nomura's jellyfish ameliorates inflammatory responses in lipopolysaccharide-stimulated RAW264.7 cells and a zebrafish model of inflammation. Biomed. Pharmacother. 100, 583–589.

Kim-Anne, L., Swapna, M., Alderete, T.L., Hasson, R.E., Adam, T.C., Joon Sung, K., Elizabeth, B., Chen, X., Greenberg, A.S., Hooman, A., 2011. Subcutaneous adipose tissue macrophage infiltration is associated with hepatic and visceral fat deposition, hyperinsulinemia, and stimulation of NF-κB stress pathway. Diabetes 60, 2802–2809.

Kim, M.Y., Linardic, C., Obeid, L., Hannun, Y., 1991. Identification of sphingomyelin turnover as an effector mechanism for the action of tumor necrosis factor alpha and gamma-interferon. Specific role in cell differentiation. J. Biol. Chem. 266, 484–489.

Kolak, M., 2012. Expression of ceramide-metabolising enzymes in subcutaneous and intra-abdominal human adipose tissue. Lipids Health Dis. 11, 115–127.

Kolesnick, R., Golde, D.W., 1994. The sphingomyelin pathway in tumor necrosis factor and interleukin-1 signaling. Cell 77, 325–328.

Kolesnick, R.N., Krönke, M., 1998. Regulation of ceramide production and apoptosis. Annu. Rev. Physiol. 60, 643–665.

Li, J.F., Qu, F., Zheng, S.J., Wu, H.L., Liu, M., Liu, S., Ren, Y., Ren, F., Chen, Y., Duan, Z.P., 2014. Elevated plasma sphingomyelin (d18:1/22:0) is closely related to hepatic steatosis in patients with chronic hepatitis C virus infection. Eur. J. Clin. Microbiol. Infect. Dis. 33, 1725–1732.

Liang, X., Xiu, C., Liu, M., Lin, C., Chen, H., Bao, R., Yang, S., Yu, J., 2018. Platelet-neutrophil interaction aggravates vascular in fl ammation and promotes the progression of atherosclerosis by activating the TLR4/NF-kappaB pathway. J. Cell. Biochem. https://doi.org/10.1002/jcb.27844.

Lim, A., Wenk, M.R., Tong, L., 2015. Lipid-based therapy for ocular surface inflammation and disease. Trends Mol. Med. 21, 736–748.

Maceyka, M., Spiegel, S., 2014. Sphingolipid metabolites in inflammatory disease. Nature 510, 58–67.

Meikle, P.J., Wong, G., Barlow, C.K., Kingwell, B.A., 2014. Lipidomics: potential role in risk prediction and therapeutic monitoring for diabetes and cardiovascular disease. Pharmacol. Ther. 143, 12–23.

Memon, R.A., Holleran, W.M., Moser, A.H., Seki, T., Uchida, Y., Fuller, J., Shigenaga, J.K., Grunfeld, C., Feingold, K.R., 1998. Endotoxin and cytokines increase hepatic sphingolipid biosynthesis and produce lipoproteins enriched in ceramides and sphingomyelin. Arterioscler. Thromb. Vasc. Biol. 18, 1257–1265.

Murph, M., Tanaka, T., Pang, J., Felix, E., Liu, S., Trost, R., Godwin, A.K., Newman, R., Mills, G., 2007. Liquid Chromatography Mass Spectrometry for Quantifying Plasma Lysophospholipids: Potential Biomarkers for Cancer Diagnosis, vol. 433. pp. 1–25.

Newcomb, B., Rhein, C., Mileva, I., Ahmad, R., Clarke, C.J., Snider, J., Obeid, L.M., Hannun, Y.A., 2018. Identification of an acid sphingomyelinase ceramide kinase pathway in the regulation of the chemokine CCL5. J. Lipid Res. 59, 1219–1229.

Qi, J., Tan, C.K., Hashimi, S.M., Zulfiker, A.H., Good, D., Wei, M.Q., 2014. Toad glandular secretions and skin extractions as anti-inflammatory and anticancer agents. Evid. Based Complement. Alternat. Med. 312684–312692 2014.

Ryu, S.J., Choi, H.S., Yoon, K.Y., Lee, O.H., Kim, K.J., Lee, B.Y., 2015. Oleuropein suppresses LPS-induced inflammatory responses in RAW 264.7 cell and zebrafish. J. Agric. Food Chem. 63, 2098–2105.

Schütze, Stefan, Potthoff, Karin, Machleidt, Thomas, Berkovic, Dinko, Wiegmann, Katja, 1992. TNF activates NF-κB by phosphatidylcholine-specific phospholipase C-induced "Acidic" sphingomyelin breakdown. Cell 71, 765–776.

Schwandner, R., Wiegmann, K.,., Bernardo, K.,., Kreder, D.,., Kronke, M., 1998. TNF receptor death domain-associated proteins TRADD and FADD signal activation of acid sphingomyelinase. J. Biol. Chem. 273, 5916–5922.

Snider, S.A., Margison, K.D., Ghorbani, P., LeBlond, N.D., O'Dwyer, C., Nunes, J.R.C., Nguyen, T., Xu, H., Bennett, S.A.L., Fullerton, M.D., 2018. Choline transport links macrophage phospholipid metabolism and inflammation. J. Biol. Chem. 293, 11600–11611.

Titz, B., Gadaleta, R.M., Lo Sasso, G., Elamin, A., Ekroos, K., Ivanov, N.V., Peitsch, M.C., Hoeng, J., 2018. Proteomics and lipidomics in inflammatory bowel disease research: from mechanistic insights to biomarker identification. Int. J. Mol. Sci. 19. https://doi.org/10.3390/ijms19092775.

Venable, M.E., Lee, J.Y., Smyth, M.J., Bielawska, A., Obeid, L.M., 1995. Role of ceramide in cellular senescence. J. Biol. Chem. 270, 30701–30708.

Wang, Y., Tu, Q., Yan, W., Xiao, D., Zeng, Z., Ouyang, Y., Huang, L., Cai, J., Zeng, X., Chen, Y.J., Liu, A., 2015. CXC195 suppresses proliferation and inflammatory response in LPS-induced human hepatocellular carcinoma cells via regulating TLR4-MyD88-TAK1-mediated NF-kappaB and MAPK pathway. Biochem. Biophys. Res. Commun. 456, 373–379.

Wenk, M.R., 2005. The emerging field of lipidomics. Nat. Rev. Drug Discov. 4, 594–610.

Yang, K., Han, X., 2016. Lipidomics: techniques, applications, and outcomes related to biomedical sciences. Trends Biochem. Sci. 41, 954–969.

Yang, L., Zhou, X., Huang, W., Fang, Q., Hu, J., Yu, L., Ma, N., Zhang, W., 2017. Protective effect of phillyrin on lethal LPS-induced neutrophil inflammation in zebrafish. Cell. Physiol. Biochem. 23, 2074–2087.

Yoo, J.M., Kim, J.H., Park, S.J., Kang, Y.J., Kim, T.J., 2012. Inhibitory effect of eriodictyol on IgE/Ag-induced type I hypersensitivity. Biosci. Biotechnol. Biochem. 76, 1285–1290.

Zhang, B., Wang, X., Li, Y., Wu, M., Wang, S.Y., Li, S., 2018. Matrine is identified as a novel macropinocytosis inducer by a network target approach. Front. Pharmacol. 9. https://doi.org/10.3389/fphar.2018.00010.

Zhang, Y., Yuan, B., Takagi, N., Wang, H., Zhou, Y., Si, N., Yang, J., Wei, X., Zhao, H., Bian, B., 2019. Comparative analysis of hydrophilic ingredients in toad skin and toad venom using the UHPLC-HR-MS/MS and UPLC-QqQ-MS/MS methods together with the anti-inflammatory evaluation of indolealkylamines. Molecules 24. https://doi.org/10.3390/molecules24010086.

Zhao, Y.Y., Cheng, X.L., Lin, R.C., 2014. Chapter one–lipidomics applications for discovering biomarkers of diseases in clinical chemistry. Int. Rev. Cell Mol. Biol. 313, 1–26.

Zheng, J., Wu, M., Wang, H., Li, S., Wang, X., Li, Y., Wang, D., Li, S., 2018. Network pharmacology to unveil the biological basis of health-strengthening herbal medicine in cancer treatment. Cancers 10, 461–483.

Zong, X., Song, D., Wang, T., Xia, X., Hu, W., Han, F., Wang, Y., 2015. LFP-20, a porcine lactoferrin peptide, ameliorates LPS-induced inflammation via the MyD88/NF-kappaB and MyD88/MAPK signaling pathways. Dev. Comp. Immunol. 52, 123–131.